Published in final edited form as:

J Immunol. 2019 January 15; 202(2): 591–597. doi:10.4049/jimmunol.1801196.

Extent of MHC clustering regulates selectivity and effectiveness of T-cell responses*

Nadia Anikeeva[1)], **Nicholas O. Fischer**[2)], **Craig D. Blanchette**[2),3)], and **Yuri Sykulev**[1),#]

[1)]Department of Microbiology and Immunology and Sidney Kimmel Cancer Center, Thomas Jefferson University, Philadelphia

[2)]Biosciences & Biotechnology Division, Physical and Life Sciences Directorate, Lawrence Livermore National Laboratory, Livermore, CA, United States

[3)]Current Address: Genentech, 1 DNA way, South San Francisco, CA, 94080

Abstract

MHC proteins that present peptide ligands for recognition by T-cell antigen receptor (TCR) form nano-scale clusters on the cell membrane of antigen-presenting cells. How the extent of MHC clustering controls productive TCR engagement and TCR-mediated signaling has not been systematically studied. To evaluate the role of MHC clustering, we exploited nano-scale discoidal membrane mimetics (nanolipoprotein particles, or NLPs) to capture and present pMHC ligands at various densities. We examined the binding of these model membrane clusters to the surface of live human $CD8^+$ T cells and the subsequent triggering of intracellular signaling. The data demonstrate that the proximity of pMHC ligands, high association rate of CD8-MHC interactions, and relatively long lifetime of cognate TCR-pMHC complexes emerge as essential parameters explaining the significance of MHC clustering. Rapid rebinding of CD8 to MHC suggests a dual role of CD8 in facilitating the T cells' hunt for a rare foreign pMHC ligand and the induction of rapid T-cell response. Thus, our findings provide a new understanding of how MHC clustering influences multivalent interactions of pMHC ligands with CD8 and TCR on live T cells that regulate antigen recognition, kinetics of intracellular signaling, and the selectivity and efficiency of T-cell responses.

Keywords

antigen presentation; peptide-MHC (pMHC) clustering; TCR-mediated Ca^{2+} signaling; selectivity of T cell responses; nanolipoprotein particle (NLP)

Introduction

MHC proteins bearing peptide antigens form nano-scale clusters on the surface of antigen-presenting cells (1–3). The clusters contain 2–20 of tightly packed MHC molecules (3–5).

*This work was supported by National Institute of Health (R21 AI113819 to Y.S., which includes subcontract DE-AC52–07NA27344 to LLNL, and in part R01 CA217714 to Y.S.).

#Corresponding author: Yuri Sykulev, Department of Microbiology and Immunology, and Medical Oncology, Kimmel Cancer Center, Thomas Jefferson University, 233S 10th St, BLSB 706, Philadelphia, PA 19107, Phone: 215-503-4530, Yuri.Sykulev@Jefferson.edu.

While it is thought that MHC clustering could control antigen presentation and T-cell responses (6), rigorous analysis of the effect of MHC clustering has been challenging. Available approaches (1, 7) do not allow to systematically evaluate how the clusters' size, density and composition influence TCR engagement and triggering of TCR-mediated signaling.

To model membrane pMHC clusters, we utilized nanolipoprotein particles containing functional nickel-chelating lipids (NiNLPs) allowing conjugation of His-tagged proteins (8, 9). NLPs are nano-scale discoidal membrane mimetics that are readily self-assembled upon mixing purified lipids and apolipoproteins, and provide a versatile platform for in vitro and in vivo applications (10–12). The density of the attached proteins can be reliably controlled by changing the percentage of nickel-chelating lipids in the NiNLP bilayer. These combined attributes make NiNLPs an ideal platform to evaluate how pMHC clustering affect antigen recognition and T-cell signaling.

Here, we analyze how the density of stimulatory (cognate) and non-stimulatory (non-cognate or self) pMHC ligands within model membrane clusters influences their equilibrium binding and association kinetics with live CTL as well as the induction of TCR-induced Ca^{2+} signaling. The latter controls expression of three quarter of the genes involving in T cell activation (13).

Our results demonstrate that the density of pMHCs, but not just their numbers, regulates multivalent interactions of the model pMHC clusters with TCR and CD8 on the T cells. Elucidating the role of MHC clustering provided basis for understanding of how variations in MHC clustering regulates antigen recognition and efficiency of T-cell responses against cancerous and virus-infected cells.

MATERIALS AND METHODS

Cells

Human CTL clone 68A62 recognizing HIV-derived peptide ILKEPVHGV (IV9) bound to HLA-A2 class I MHC (14) was a kind gift from B. D. Walker. Human CTL clone CER43 specific for influenza matrix protein peptide GILGFVFTL (GL9) in context with HLA-A2 (15, 16) was kindly provided by A. Lanzavecchia. The peptides IV9 and GL9 were generous gift from H.N. Eisen. The LLFGYPVYV (Tax) peptide from human T lymphotropic virus type 1 (17) was synthesized by Research Genetics, Inc.

Production of soluble MHC

"Empty" soluble HLA-A2 protein with intact and mutant CD8 binding site was produced in S2 cells and was purified from the culture supernatant as described elsewhere (18, 19). A245V mutation significantly diminishes interaction of HLA-A2mut protein with CD8 (20, 21).

Preparation of pMHC/NiNLP conjugates

Preparation of NiNLPs has been previously described in detail (9–11). pHLA-A2/NiNLP conjugate formation was driven by the interaction between the His_6-tag of pHLA-A2 and

NLPs functionalized with lipids bearing nickel-charged nitrilotriacetic acid (NiNTA) headgroups. NiNLPs were mixed with pHLA-A2 ligands at various molar ratios in DPBS buffer at final concentration of 500 nM. The mixtures were incubated at room temperature for 10 min and diluted with DPBS containing 1% BSA to achieve the required NiNLP concentrations.

Equilibrium binding of pMHC/NiNLP to T cells

68A62 or CER43 $CD8^+$ T cells were incubated with increasing amounts of freshly prepared pHLA-A2/NiNLP conjugates at a pHLA-A2-to-NiNLP ratio of 10:1 or 30:1. The mixtures were incubated with live T cells for 1 hour at the indicated temperature and the cell fluorescence was immediately measured by a Flow Cytometer. The NiNLP loaded with non-cognate Tax-HLA-A2mut protein and unconjugated NiNLP were used to measure background binding. The avidity of interactions was calculated with the GraphPad Prizma 7 program using the law of mass action:

$$Y=B_{max} * X/(K_d + X) \quad (1)$$

where Y is the MFI measured at concentration of pHLA-A2/NiNLP equal X; B_{max} is the maximum specific binding (plateau value) and K_d is an apparent equilibrium binding constant.

Binding kinetics of pMHC/NiNLP to T cells

CTL at a density of 10^7cells/ml were combined with the conjugates at 25 nM or 5 nM, and the mixture was incubated at different temperatures in DPBS/1% BSA. At designated time points, 10 μl of the mixture was diluted in 200 μl of chilled buffer, and the cell fluorescent intensities were immediately recorded using a Flow Cytometer. NiNLPs loaded with non-cognate Tax-HLA-A2mut protein or unconjugated NiNLPs were used to measure the background binding. The background subtracted data were fitted to an exponential equation with the GraphPad Prizm 7 program using one- or two-phase exponential models:

$$A(t) = \sum_{i=1}^{n} A_i \left(1 - \exp(-t\, k_i)\right) \quad (2)$$

where $k_i=1/\tau_i$ and A_i, k_i, and τ_i are the amplitude, rate and time constants, respectively.

To distinguish between one- and two-phase exponential models, an extra sum-of-squares F test was applied.

Measuring the kinetics of CTL Ca^{2+} signaling

CTL were loaded with Fluo-4 Ca^{2+} sensitive fluorophore as previously described (20, 22). Time-dependent changes in intracellular fluorescent intensity were measured using a BD LSR II Flow Cytometer. After measuring the background fluorescence, freshly prepared pHLA-A2/NiNLP were promptly added to 1 ml of the cell suspension (10^6 cells/ml). The

data were analyzed with FlowJo software. Non-cognate pHLA-A2/NiNLP conjugate were used as a negative control.

RESULTS

Preparation and characterization of pMHC/NiNLP

Nanolipoprotein particles (NLPs) were assembled to include a functional nickel-chelating lipid (NiNLPs) allowing for conjugation of His_6-tagged proteins (Fig. 1A). The surface density of attached proteins can be reliably controlled by varying the percentage of nickel-chelating lipids in the NLP bilayer. The conjugation was assessed by analytical size exclusion chromatography (aSEC) at different pHLA-A2:NiNLP ratios (Fig. 1B). Analysis of the integrated area under the pMHC/NiNLP peak allowed to determine pHLA-A2:NiNLP molar ratio for each NiNLP containing distinct amount of nickel-chelating lipids (Fig. 1C). For the experiments described here, we choose NLPs containing 5 mol% and 25 mol% of functional nickel-chelating lipid that bear 10 and 30 pHLA-A2 molecules, respectively.

The diameters of NiNLPs and MHC molecules are circa 20 nm (9, 10) and 5 nm (23, 24), respectively. As such, 15 pMHCs can be captured on each bilayer surface of the nanoparticle having 25 mol% of NiNTA. These NiNLPs, produce high-density pMHC/NiNLP with close proximity between pMHC proteins, and reflect the clustering of pMHC found at the surface of live cells (3). NiNLPs containing 5 mol% of NiNTA immobilized 10 molecules per NiNLP, which are herein referred to as low-density pMHC/NiNLP.

To evaluate multivalent receptor-ligand interactions between model pMHC membrane clusters and live CD8+ T cells, we utilized NiNLPs containing fluorescent-labeled Apo protein, which allowed us to measure the amount of membrane-bound pHLA-A2/NiNLPs by flow cytometry.

Equilibrium binding of pHLA-A2/NiNLPs with different stoichiometry to live T cells

To calculate apparent affinity constants (Kapp) for pMHC/NiNLP binding to live T cells, we utilized the following pMHC ligands: (i) cognate (strong agonist), (ii) non-cognate (“self”), and (iii) the agonist ligands containing HLA molecules with mutated CD8 binding site. The last two ligands were analyzed to dissect contribution of CD8-pMHC and TCR-pMHC interactions to multivalent binding.

The high-density pHLA-A2/NiNLPs (30:1) bound to live 68A62 CTL with higher apparent affinity compared to low-density pHLA-A2/NiNLPs (10:1) regardless of the kind of pHLA-A2 and temperature (Fig. 2 and Table 1). Binding experiments with CER43 CTL produced similar results (data not shown). To quantify the difference, we introduced an enhancement factor, which was calculated as a ratio between apparent binding constants for low- and high-density pHLA-A2/NiNLPs. The analysis revealed that the enhancement factor for the non-cognate conjugates was much higher than for the mutated and intact cognate conjugates (Table 1); the difference was even more profound with temperature increase. Indeed, the amount of cell-bound low-density non-cognate pHLA-A2/NiNLP was barely detectable at 37°C as opposed to high-density pHLA-A2/NiNLP (Fig. 2C and D). In contrast to non-cognate conjugates, elevated temperature enhanced the binding of high- and low-density

cognate conjugates with mutated CD8 binding site, by 1.6- and 4.14-fold, respectively (Table 1) providing evidence for the opposite effect of the temperature changes on multivalent CD8-MHC and TCR-pMHC interactions. In accord with these findings, the apparent binding constant of low-density cognate pHLA-A2/NiNLPs increased by 2-fold after the temperature was raised from 4°C to 22–24°C, while the binding of high-density cognate pHLA-A2/NiNLPs showed only a slight temperature dependence (Table 1). These data provide compelling evidence that the pMHC density within model membrane clusters strongly affects binding to the T-cell surface and that CD8-MHC interactions play a major role in determining contribution of self pMHC to antigen recognition by T cells. Importantly, at 37°C low density non-cognate pMHC model clusters essentially do not bind to the T-cell surface (Fig. 2D) indicative of higher selectivity of T-cell responses at physiological conditions.

The observed effects may be attributed exclusively to a larger number of pHLA-A2 proteins displayed on high density pHLA-A2/NiNLPs, i.e. higher multivalency of the nanoparticles. To decouple the role of density and valency in the binding of model membrane clusters, we utilized pMHC/quantum dots (pMHC/QD(520)). The proximity between the pMHCs on QD (21) was similar to that for pMHCs presented on high density NiNLPs (see above), and the number of the ligands per QD nanoparticle capable to interact with TCR/CD8 was much the same as for low density pMHC/NiNLPs. Thus, pHLA-A2/QD conjugates have significantly lower valency but similar density when compared to high-density pMHC/NiNLPs. We found that both cognate and non-cognate pHLA-A2/QD conjugates were bound to the surface of activated T cells (Supplemental Fig. 1). The difference between Kapp as well as normalized binding plateau values were similar to those observed for cognate and non-cognate high-density but not low density pHLA-A2/NiNLPs (Table 1). Thus, the density, but not multivalency was found to affect the efficiency of MHC-CD8 interactions and controls the ability of non-cognate conjugates to bind to T-cell surface.

Despite the higher expression level of CD8 relative to TCR/CD3 on the surface of T cells (25)(Supplemental Table 1), the plateau values of high-density non-cognate pHLA-A2/NiNLP binding were lower than the maximum of the binding for cognate pHLA-A2/NiNLPs (Fig. 2A and Table 1). This suggests that merely a fraction of CD8 molecules on the T-cell surface were capable of interacting with non-cognate pHLA-A2/NiNLPs. The results are consistent with previous findings demonstrating that only a fraction of CD8 molecules on the surface of activated, but not naïve T cells, are co-clustered with the TCR (26). To support this notion, we compared binding of cognate and non-cognate conjugates to the surface of activated and naïve 2C T cells. While cognate SIYRYYGL-K^b/NiNLPs interacted equally well with the cell surface of naïve and activated 2C cells, the binding of non-cognate SIINFEKL-K^b/NiNLP to naïve T cells was barely detectable despite similar level of expression of CD8 co-receptor on both naïve and activated T cells (Supplemental Fig. 2).

Effect of pMHC density on the kinetics of pMHC/NiNLP binding

Multivalent interactions typically require a long time (many hours) to achieve equilibrium, while interaction between CTL and target cells is very dynamic process that occurs very rapidly (minutes). To determine how pMHC cluster density influences the kinetics of their

interactions with CD8 T cells, we compared the binding kinetics of various pMHC/NiNLPs conjugates to CTL surface.

For both high- and low-density cognate conjugates, biphasic time courses with similar contribution of the fast phase were observed (Fig. 3 and Table 2). However, comparison of the time constants for high- and low-density pHLA-A2/NiNLPs indicated that the latter bound to live T cells with slower kinetics. To understand these differences, the binding of noncognate and mutated cognate pMHC/NiNLPs conjugates was analyzed. The time-courses of both high and low density cognate pHLA-A2mut/NiNLPs were monophasic with very similar large time constants and low amplitudes. In contrast, the binding kinetics of low- and high-density non-cognate pMHC/NiNLPs was very different. The association of high-density non-cognate pHLA-A2/NiNLPs was biphasic with time constant values close to that of the cognate conjugate. In contrast, real time association curve of low-density non-cognate pMHC/NLPs was monophasic with relatively large time constant. This indicates that CD8-MHC interaction is responsible for the rapid kinetics observed for high density cognate pHLA-A2/NiNLP interaction with CD8 T cell surface.

To evaluate the effect of valency versus proximity of the pHLA-A2 ligands, the binding kinetics of QD/pMHC(520) was analyzed. As evident from Supplemental Fig. 1, the association kinetics of both cognate and non-cognate pHLA-A2/QD was very similar resembling the binding kinetics of the high-density pHLA-A2/NiNLP conjugates (Fig. 3) despite lower valency of pHLA-A2/QD conjugates. These data provide evidence that the proximity of the pMHC ligands rather than the valency has a stronger impact on binding kinetics of pMHC/NiNLPs with various pMHC densities.

The role of pMHC density in regulating the kinetics of TCR-mediated Ca^{2+} signaling

To evaluate the effects of pMHC ligand density and MHC mutation that weaken CD8-MHC interactions on TCR-mediated signaling, we measured intracellular calcium flux induced by various pMHC/NiNLPs in real time. Induction of Ca^{2+} signaling by pMHC/NiNLPs occurs very rapidly, and the assay conditions preclude formation of cell-cell conjugates and allow the evaluation integrated responses by individual T cells. For comparison reasons, the changes in intracellular Ca^{2+} level were measured at concentration of pMHC/NiNLP conjugates close to the apparent K_D of their interactions with the T cells.

Figure 4A shows that high-density cognate pHLA-A2/NiNLPs were superior in the induction of robust Ca^{2+} signaling as opposed to low-density pHLA-A2/NiNLP. To further explore the role of the proximity between pHLA-A2, we utilized high density pMHC/NiNLP loaded with a mixture of cognate and non-cognate pMHC ligands. The total number of pMHC per particle was kept the same, but the number of cognate pMHC was adjusted to that displayed on the low-density pMHC/NiNLP. Figure 4B shows that the total MHC density, but not the density of cognate pMHC controls the induction of the robust Ca^{2+} signaling. When cognate pHLA-A2 were replaced with cognate pHLA-A2mut, the signaling kinetics was significantly diminished (Fig. 4C). This effect became even more pronounced when the experiment repeated with the low-density conjugates (Fig. 4C). These data demonstrate that high density of pMHC molecules capable of interacting with CD8 within

the membrane MHC clusters facilitates the kinetics of clustered pMHC interactions with the T cell surface that regulates the kinetics and magnitude of Ca^{2+} signaling.

DISCUSSION

The major finding of this study is that the density of pMHC molecules displayed on model membrane clusters strongly influences their binding to live CTL and the kinetics of intracellular Ca^{2+} signaling. Importantly, the binding of pMHC/NiNLPs to the T-cell surface is regulated by both TCR-pMHC and CD8-MHC multivalent interactions, each contributing to the binding in a unique way. While CD8-MHC interactions are characterized by high association rate constant and very short lifetime, TCR typically interacts with cognate pMHC with much slower rate but form more stable complexes. Although CD8-MHC and TCR-pMHC interactions in vitro have been previously studied (27, 28), the contribution of these interactions on multivalent binding at the cell membrane have not yet been investigated. Here we have shown that close proximity between the pMHC ligands involved in the multivalent interactions favors rebinding of the ligands to CD8 co-receptor that, along with the higher stability of the TCR-pMHC bonds, control the strength of pMHC/NiNLP association with the cell surface. Therefore, each interaction regulates apparent affinity of the multivalent binding in a different way. Consistent with this, computer simulation of bivalent ligand interactions with membrane bound molecules have shown that the highest gain in apparent affinity of the interactions is achieved when the interaction of monovalent ligand with the receptor have a rapid kinetic constant of association with moderate life time of the complex (29). Thus, the proximity of pMHC ligands, high association rate of CD8-MHC interactions, and relatively long lifetime of cognate TCR-pMHC complexes emerges as essential parameters explaining significance of MHC clustering in controlling multivalent interactions of pMHC membrane clusters with TCR/CD8 proteins on live T cells.

Analysis of equilibrium parameters of multivalent binding suggests an essential role for CD8-MHC interactions in the rapid scanning of target cell surface to identify a rare pMHC ligand. On the other hand, rapid rebinding of CD8 to MHC facilitates binding kinetics of dense clusters to the T-cell surface, which in turn facilitates the kinetics of intracellular signaling and T-cell response. Therefore, CD8 plays a dual role facilitating the “hunt” by T cells for a rare or recently presented foreign pMHC ligand and rapid T-cell response.

The important role of MHC density became even more apparent upon comparing the kinetics of Ca^{2+} signaling in T cells induced by high- and low-density cognate pMHC/NLPs (Fig. 4A). The superior potency of the high-density pMHC/NLPs was still evident when the number of cognate pMHC was decreased to match that presented on low-density conjugates with all others being replaced by non-cognate pMHC (Fig. 4B). These data provide further evidence that self pMHC within high-density pMHC clusters facilitate recognition of a small amount of cognate pMHC ligands by CD8 T cells (20, 21, 30). Close proximity of CD8 co-receptors, which are bound to foreign and self MHC molecules within high density clusters, may initiate p56lck trans-phosphorylation that also induces activation of TCRs bound to self pMHC ligands within the TCR/CD8 cluster, a mechanism that has been referred to as signal spread (20). Cooperation of cognate and non-cognate pMHC within high density membrane

clusters facilitates rapid accumulation of intracellular Ca^{2+} in CTL that is linked to effective delivery of cytolytic granules and potent cytolytic response (31, 32).

The cooperation of cognate and self pMHCs has been previously delineated (20, 33), and clustering of self pMHCs has been shown to be particularly important as they are always present in a large excess relative to foreign pMHC on antigen-presenting cells (21, 34, 35). Thus, in the dense nanocluster self pMHC proteins could effectively facilitate recognition of even a single foreign pMHC ligand within the same cluster resulting in a robust T cell response (20, 36). In contrast, poor clustering of MHC proteins on transformed cells could contribute to inefficient potency of T cells to attack on cancer cells.

The significance of close proximity of pMHC ligands within MHC clusters is also evident from our failure to observe cooperation of cognate and self pMHC ligands incorporated into bilayers (Anikeeva, Somersalo, Dustin, Sykulev, unpublished). Even with the bilayers containing artificial barriers that limit diffusion of pMHCs (37–39), it is impossible to achieve the pMHC density similar to that observed for pMHC clusters assembled on nanoparticles or those presented on the cell membrane (5, 21). The density of pMHC on nanoparticles is significantly higher when compared to planar bilayers where pMHC ligands could not be positioned close enough to each other to cooperate during TCR and co-receptor engagement.

Upon delivery to the surface, pMHC ligands appear as large patches containing about 100–150 pMHC molecules (40), which are relatively short-lived with half-lives of around 30 seconds (41). The pMHC molecules then diffuse away from the patches generating smaller clusters and individual molecules (40). The appearance and subsequent disaggregation of a large pMHC clusters at the cell surface is a continuous process ensuring sustained presentation of newly generated peptides (42). Comparison of the potency of high- and low-density pMHC/NiNLPs suggests that the most efficient recognition of newly processed peptides occurs within a large MHC membrane clusters. This is essential for early detection of infected cells by CTL during acute viral infection and initial containment of the infection. In contrast, low-density pMHC clusters possess much lower efficiency to stimulate T-cell responses due to diminished ability of self pMHC ligands to facilitate recognition of cognate pMHC (Fig. 2D). The clustering of cell surface receptors and their ligands involved in multivalent receptor-ligand interactions may also allow the formation of different patterns of engaged receptors, each possibly linked to a particular cellular response and efficacy. Thus, clustering of immune receptors appears to be an essential mechanism regulating T cell responses.

Because TCR and CD8 on naïve T cells are not co-clustered (26, 43), antigen recognition by naïve T cells appears to be less efficient (44). This is expected to favor T cells responses to strong peptide epitopes enhancing specificity and diminishing cross-reactivity. During chronic infection, activated T cells whose TCR and CD8 are co-clustered respond more efficiently to clustered pMHC on APC allowing the detection of minute amounts of viral peptides as well as weak agonist peptides and mutated viral peptides displayed on the infected cells. Thus, responses of activated T cells are more sensitive, but less selective (i.e., could target a wider range of peptide antigens). These considerations are consistent with the

difference in the order of TCR and CD8 engagement on the surface of activated T cells described here and naïve T cells previously studied by Zhu and colleagues (45).

We have previously shown that MHC clusters on APC may include heterotypic membrane proteins such as ICAM-1, a ligand for LFA-1 integrin, which augment the sensitivity of the T cell response (1). This is consistent with our recent findings showing that integrin-mediated signaling regulates the efficiency of proximal signaling in cytotoxic lymphocytes (46, 47). Productive engagement of other receptors leads to recruitment of adaptor and signaling proteins to the TCR containing clusters and formation of signalosomes (48) that integrate receptor-mediated signaling. Thus, clustering of immune receptors and proximal signaling proteins represent a highly sensitive regulatory mechanism that likely controls the balance of positive and negative signaling to ensure efficient responses against legitimate targets and to avoid overstimulation and the induction of T cell death.

Supplementary Material

Refer to Web version on PubMed Central for supplementary material.

ACKNOWLEDGMENTS -

We are grateful to Bruce Walker and Antonio Lanzavecchia for providing human CD8+ T-cell clones. We also thank Flow Cytometry Facility of the Sidney Kimmel Cancer Center for excellent technical support.

Abbreviations used in this article:

HLA	human leukocyte antigen
MHC	Major Histocompatibility Complex
TCR	T cell receptor
ICAM-1	intercellular adhesion molecule 1
LFA-1	lymphocyte function-associated antigen 1
pMHC	peptide-MHC
NiNLP	nanolipoprotein particles containing functional nickel-chelating lipids
CTL	cytotoxic T lymphocytes
BSA	bovine serum albumin
aSEC	analytical size exclusion chromatography
QD	quantum dots
APC	antigen-presenting cell
p56lck	lymphocyte-specific protein tyrosine kinase

REFERENCES

1. Lebedeva T, Anikeeva N, Kalams SA, Walker BD, Gaidarov I, Keen JH, and Sykulev Y. 2004 Major histocompatibility complex class I-intercellular adhesion molecule-1 association on the surface of target cells: implications for antigen presentation to cytotoxic T lymphocytes. Immunology 113: 460–471. [PubMed: 15554924]
2. Lebedeva T, Dustin ML, and Sykulev Y. 2005 ICAM-1 co-stimulates target cells to facilitate antigen presentation. Curr Opin Immunol 17: 251–258. [PubMed: 15886114]
3. Ferez M, Castro M, Alarcon B, and van Santen HM. 2014 Cognate peptide-MHC complexes are expressed as tightly apposed nanoclusters in virus-infected cells to allow TCR crosslinking. J Immunol 192: 52–58. [PubMed: 24307729]
4. Abbas AK, Dorf ME, Karnovsky MJ, and Unanue ER. 1976 The distribution of Ia antigens on the surfaces of lymphocytes. J Immunol 116: 371–378. [PubMed: 1082455]
5. Hwang J, Gheber LA, Margolis L, and Edidin M. 1998 Domains in cell plasma membranes investigated by near-field scanning optical microscopy. Biophys J 74: 2184–2190. [PubMed: 9591645]
6. Sykulev Y 2010 Changing separating distances between immune receptors as a sensitive mechanism regulating T-cell activation. Self Nonself 1: 67–68. [PubMed: 21318086]
7. Anderson HA, Hiltbold EM, and Roche PA. 2000 Concentration of MHC class II molecules in lipid rafts facilitates antigen presentation. Nat Immunol 1: 156–162. [PubMed: 11248809]
8. Blanchette CD, Segelke BW, Fischer N, Corzett MH, Kuhn EA, Cappuccio JA, Benner WH, Coleman MA, Chromy BA, Bench G, Hoeprich PD, and Sulchek TA. 2009 Characterization and purification of polydisperse reconstituted lipoproteins and nanolipoprotein particles. Int J Mol Sci 10: 2958–2971. [PubMed: 19742178]
9. Fischer NO, Blanchette CD, Chromy BA, Kuhn EA, Segelke BW, Corzett M, Bench G, Mason PW, and Hoeprich PD. 2009 Immobilization of His-tagged proteins on nickel-chelating nanolipoprotein particles. Bioconjug Chem 20: 460–465. [PubMed: 19239247]
10. Blanchette CD, Fischer NO, Corzett M, Bench G, and Hoeprich PD. 2010 Kinetic analysis of his-tagged protein binding to nickel-chelating nanolipoprotein particles. Bioconjug Chem 21: 1321–1330. [PubMed: 20586461]
11. Fischer NO, Infante E, Ishikawa T, Blanchette CD, Bourne N, Hoeprich PD, and Mason PW. 2010 Conjugation to nickel-chelating nanolipoprotein particles increases the potency and efficacy of subunit vaccines to prevent West Nile encephalitis. Bioconjug Chem 21: 1018–1022. [PubMed: 20509624]
12. Weilhammer D, Dunkle AD, Blanchette CD, Fischer NO, Corzett M, Lehmann D, Boone T, Hoeprich P, Driks A, and Rasley A. 2017 Enhancement of antigen-specific CD4(+) and CD8(+) T cell responses using a self-assembled biologic nanolipoprotein particle vaccine. Vaccine 35: 1475–1481. [PubMed: 28214044]
13. Feske S, Giltnane J, Dolmetsch R, Staudt LM, and Rao A. 2001 Gene regulation mediated by calcium signals in T lymphocytes. Nat Immunol 2: 316–324. [PubMed: 11276202]
14. Tsomides TJ, Walker BD, and Eisen HN. 1991 An optimal viral peptide recognized by $CD8^+$ T cells binds very tightly to the restricting class I major histocompatibility complex protein on intact cells but not to the purified class I protein. Proc. Natl. Acad. Sci. USA 88: 11276–11280. [PubMed: 1722325]
15. Gotch F, Rothbard J, Howland K, Townsend A, and McMichael A. 1987 Cytotoxic T lymphocytes recognize a fragment of influenza virus matrix protein in association with HLA-A2. Nature 326: 881–882. [PubMed: 2437457]
16. Valitutti S, Muller S, Dessing M, and Lanzavecchia A. 1996 Different responses are elicited in cytotoxic T lymphocytes by different levels of T cell receptor occupancy. J. Exp. Med 183: 1917–1921. [PubMed: 8666949]
17. Elovaara I, Koenig S, Brewah AY, Woods RM, Lehky T, and Jacobson S. 1993 High human T cell lymphotropic virus type 1 (HTLV-1)-specific precursor cytotoxic T lymphocyte frequencies in patients with HTLV-1-associated neurological disease. J Exp Med 177: 1567–1573. [PubMed: 8496677]

18. Anikeeva N, Lebedeva T, Krogsgaard M, Tetin SY, Martinez-Hackert E, Kalams SA, Davis MM, and Sykulev Y. 2003a Distinct molecular mechanisms account for the specificity of two different T-cell receptors. Biochemistry 42: 4709–4716. [PubMed: 12705834]
19. Anikeeva N, Lebedeva T, Sumaroka M, Kalams SA, and Sykulev Y. 2003b Soluble HIV-specific T-cell receptor: expression, purification and analysis of the specificity. J. Immunol. Meth 277: 75–86.
20. Anikeeva N, Lebedeva T, Clapp AR, Goldman ER, Dustin ML, Mattoussi H, and Sykulev Y. 2006 Quantum dot/peptide-MHC biosensors reveal strong CD8-dependent cooperation between self and viral antigens that augment the T cell response. Proc Natl Acad Sci U S A 103: 16846–16851. [PubMed: 17077145]
21. Anikeeva N, Gakamsky D, Scholler J, and Sykulev Y. 2012 Evidence that the density of self peptide-MHC ligands regulates T-cell receptor signaling. PLoS One 7: e41466. [PubMed: 22870225]
22. Anikeeva N, Gakamsky D, and Sykulev Y. 2011 Quantum Dots as a Unique Nanoscaffold to Mimic Membrane Receptor Clustering In Nanotech World Conference. NSTI Nanotech, Boston 443–446.
23. Bjorkman PJ, Saper MA, Samraoui B, Bennett WS, Strominger JL, and Wiley DC. 1987a Structure of the human class I histocompatibility antigen, HLA-A2. Nature 329: 506–512. [PubMed: 3309677]
24. Bjorkman PJ, Saper MA, Samraoui B, Bennett WS, Strominger JL, and Wiley DC. 1987b The foreign antigen binding site and T cell recognition regions of class I histocompatibility antigens. Nature 329: 512–518. [PubMed: 2443855]
25. Gakamsky DM, Luescher IF, Pramanik A, Kopito RB, Lemonnier F, Vogel H, Rigler R, and Pecht I. 2005 CD8 kinetically promotes ligand binding to the T-cell antigen receptor. Biophys J 89: 2121–2133. [PubMed: 15980174]
26. Zhong L, Zeng G, Lu X, Wang RC, Gong G, Yan L, Huang D, and Chen ZW. 2009 NSOM/QD-based direct visualization of CD3-induced and CD28-enhanced nanospatial coclustering of TCR and coreceptor in nanodomains in T cell activation. PLoS One 4: e5945. [PubMed: 19536289]
27. Garcia CK, Scott CA, Brunmark A, Carbone FR, Peterson PA, Wilson IA, and Teyton L. 1996 CD8 enchances formation of stable T-cell receptor/MHC class I molecule complexes. Nature 384: 577–581. [PubMed: 8955273]
28. Wyer J, Willcox B, Gao G, Gerth U, Davis S, Bell J, van der Merwe P, and Jakobsen B. 1999 T cell receptor and coreceptor CD8 alphaalpha bind peptide-MHC independently and with distinct kinetics. Immunity 10: 219–225. [PubMed: 10072074]
29. Vauquelin G, and Charlton SJ. 2013 Exploring avidity: understanding the potential gains in functional affinity and target residence time of bivalent and heterobivalent ligands. Br J Pharmacol 168: 1771–1785. [PubMed: 23330947]
30. Anikeeva N, and Sykulev Y. 2011 Mechanisms controlling granule-mediated cytolytic activity of cytotoxic T lymphocytes. Immunol Res 51: 183–194. [PubMed: 22058021]
31. Beal AM, Anikeeva N, Varma R, Cameron TO, Vasiliver-Shamis G, Norris PJ, Dustin ML, and Sykulev Y. 2009 Kinetics of early T cell receptor signaling regulate the pathway of lytic granule delivery to the secretory domain. Immunity 31: 632–642. [PubMed: 19833088]
32. Sykulev Y 2010 T cell receptor signaling kinetics takes the stage. Sci Signal 3: pe50.
33. Krogsgaard M, Li QJ, Sumen C, Huppa JB, Huse M, and Davis MM. 2005 Agonist/endogenous peptide-MHC heterodimers drive T cell activation and sensitivity. Nature 434: 238–243. [PubMed: 15724150]
34. Yachi PP, Ampudia J, Gascoigne NR, and Zal T. 2005 Nonstimulatory peptides contribute to antigen-induced CD8-T cell receptor interaction at the immunological synapse. Nat Immunol 6: 785–792. [PubMed: 15980863]
35. Yachi PP, Lotz C, Ampudia J, and Gascoigne NR. 2007 T cell activation enhancement by endogenous pMHC acts for both weak and strong agonists but varies with differentiation state. J Exp Med 204: 2747–2757. [PubMed: 17954567]
36. Sykulev Y, Joo M, Vturina I, Tsomides TJ, and Eisen HN. 1996 Evidence that a single peptide-MHC complex on a target cell can elicit a cytolytic T cell response. Immunity 4: 565–571. [PubMed: 8673703]

37. Mossman KD, Campi G, Groves JT, and Dustin ML. 2005 Altered TCR signaling from geometrically repatterned immunological synapses. Science 310: 1191–1193. [PubMed: 16293763]

38. Nye JA, and Groves JT. 2008 Kinetic control of histidine-tagged protein surface density on supported lipid bilayers. Langmuir 24: 4145–4149. [PubMed: 18303929]

39. Manz BN, Jackson BL, Petit RS, Dustin ML, and Groves J. 2011 T-cell triggering thresholds are modulated by the number of antigen within individual T-cell receptor clusters. Proc Natl Acad Sci U S A 108: 9089–9094. [PubMed: 21576490]

40. Blumenthal D, Edidin M, and Gheber LA. 2016 Trafficking of MHC molecules to the cell surface creates dynamic protein patches. J Cell Sci 129: 3342–3350. [PubMed: 27466380]

41. Lavi Y, Edidin MA, and Gheber LA. 2007 Dynamic patches of membrane proteins. Biophys J 93: L35–37. [PubMed: 17631538]

42. Reits EA, Vos JC, Gromme M, and Neefjes J. 2000 The major substrates for TAP in vivo are derived from newly synthesized proteins [see comments]. Nature 404: 774–778. [PubMed: 10783892]

43. Borger JG, Zamoyska R, and Gakamsky DM. 2014 Proximity of TCR and its CD8 coreceptor controls sensitivity of T cells. Immunol Lett 157: 16–22. [PubMed: 24263053]

44. Iezzi G, Karjalainen K, and Lanzavecchia A. 1998 The duration of antigenic stimulation determines the fate of naive and effector T cells. Immunity 8: 89–95. [PubMed: 9462514]

45. Jiang N, Huang J, Edwards LJ, Liu B, Zhang Y, Beal CD, Evavold BD, and Zhu C. 2011 Two-stage cooperative T cell receptor-peptide major histocompatibility complex-CD8 trimolecular interactions amplify antigen discrimination. Immunity 34: 13–23. [PubMed: 21256056]

46. Anikeeva N, Somersalo K, Sims TN, Thomas VK, Dustin ML, and Sykulev Y. 2005 Distinct role of lymphocyte function-associated antigen-1 in mediating effective cytolytic activity by cytotoxic T lymphocytes. Proc Natl Acad Sci U S A 102: 6437–6442. [PubMed: 15851656]

47. Steblyanko M, Anikeeva N, Campbell KS, Keen JH, and Sykulev Y. 2015 Integrins Influence the Size and Dynamics of Signaling Microclusters in a Pyk2-dependent Manner. J Biol Chem 290: 11833–11842. [PubMed: 25778396]

48. Werlen G, and Palmer E. 2002 The T-cell receptor signalosome: a dynamic structure with expanding complexity. Curr Opin Immunol 14: 299–305. [PubMed: 11973126]

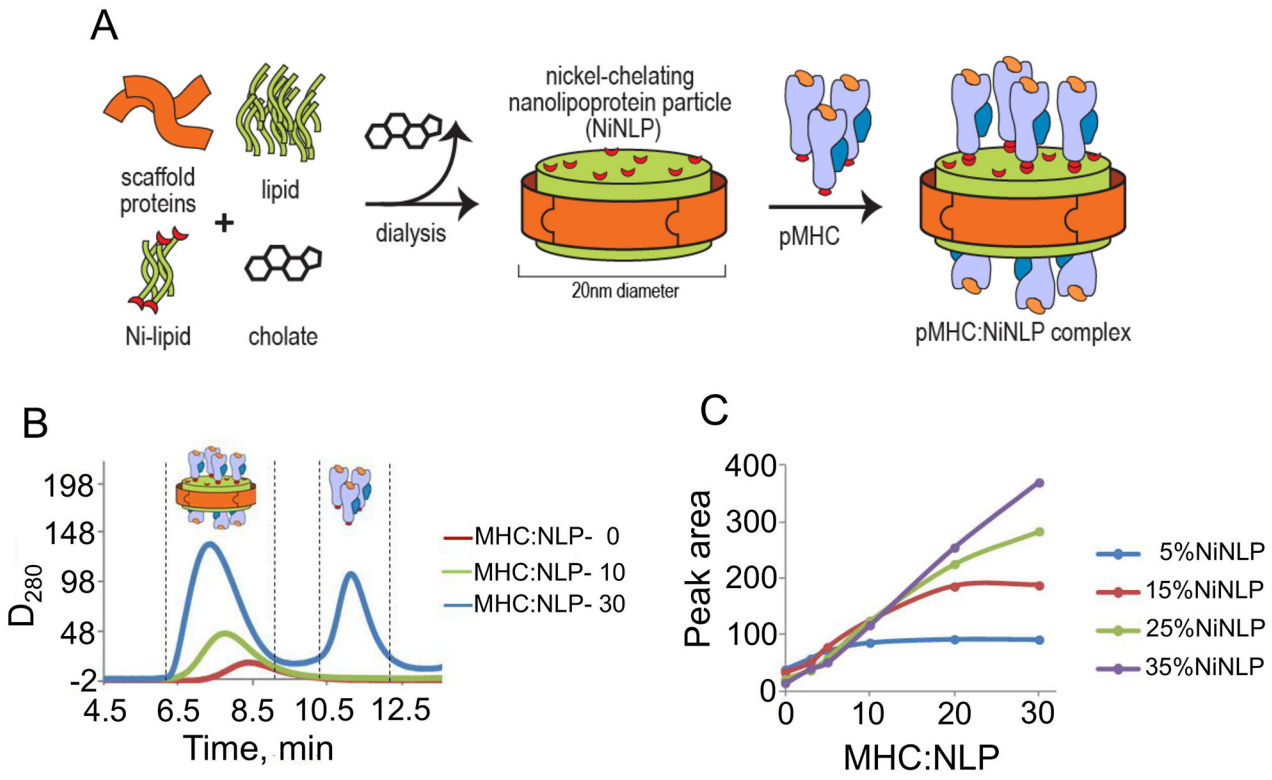

Figure 1. NiNLP assembley and non-covalent conjugation of pMHC to NiNLP platform

A. NiNLPs are assembled with a functional nickel-chelating lipid, which allows for surface conjugation of His_6-tagged proteins. **B** and **C**. Analytical size exclusion analysis (aSEC) of pMHC binding to NiNLPs. NiNLPs were incubated with pMHC at increasing pMHC:NiNLP molar ratios. An increase in molar ratio resulted in a gradual increase in the area under the main pMHC/NiNLP peak, which then plateaued at higher ratios concomitant with the appearance of a peak corresponding to free, unbound protein (**B**). The integrated area under the pMHC/NiNLP peak was analyzed as a function of the pHLA-A2:NiNLP ratio for NiNLP containing various concentrations of nickel-chelating lipids (**C**). Molar ratios for 5% and 25% of NiNLPs were found to be 10:1 and 30:1, respectively.

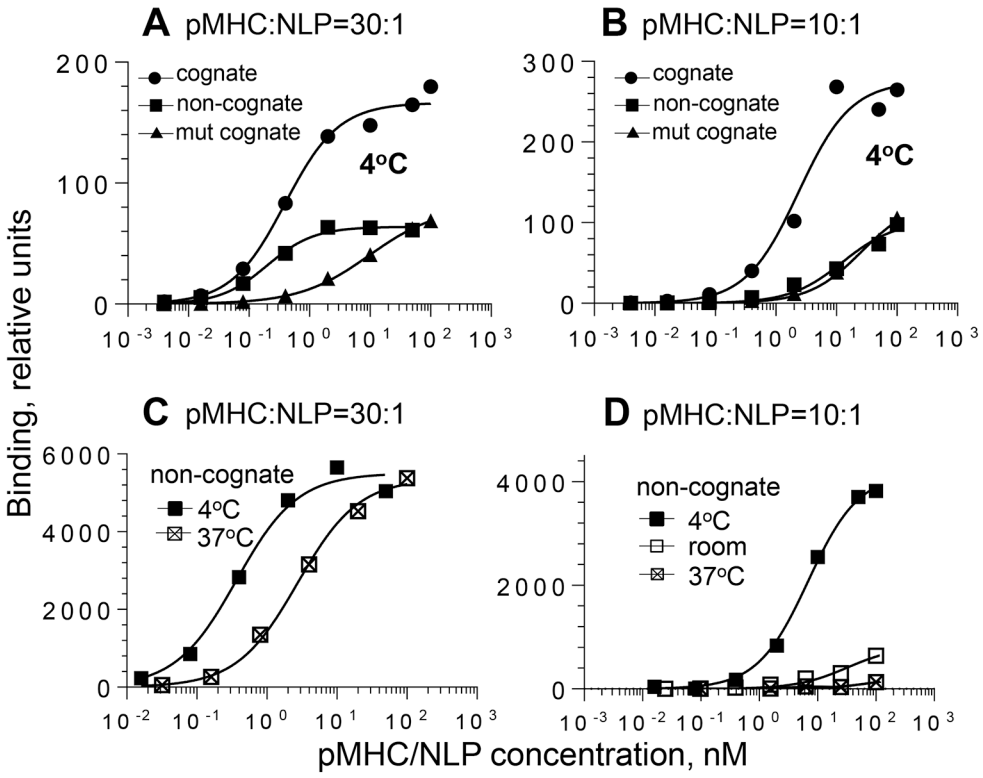

Figure 2. Equilibrium binding of pMHC/NiNLPs to the surface of live CTL.

68A62 CD8$^+$ T cells were mixed with increasing amounts of preformed pMHC/NiNLP conjugates at a pMHC-to-NLP ratio of 30:1 (**A** and **C**) or 10:1 (**B** and **D**) at indicated temperature. The data are representative graphs for binding of strong agonist IV9-HLA-A2/NiNLP at 4°C (**filled circle**), non-cognate Tax-HLA-A2/NiNLP at 4°C (**filled square**), cognate IV9-HLA-A2mut/NiNLP at 4°C (**filled triangle**), non-cognate Tax-HLA-A2/NiNLP at room temperature (**open square**), and non-cognate Tax-HLA-A2/NiNLP at 37°C (**cross-hatched square**).

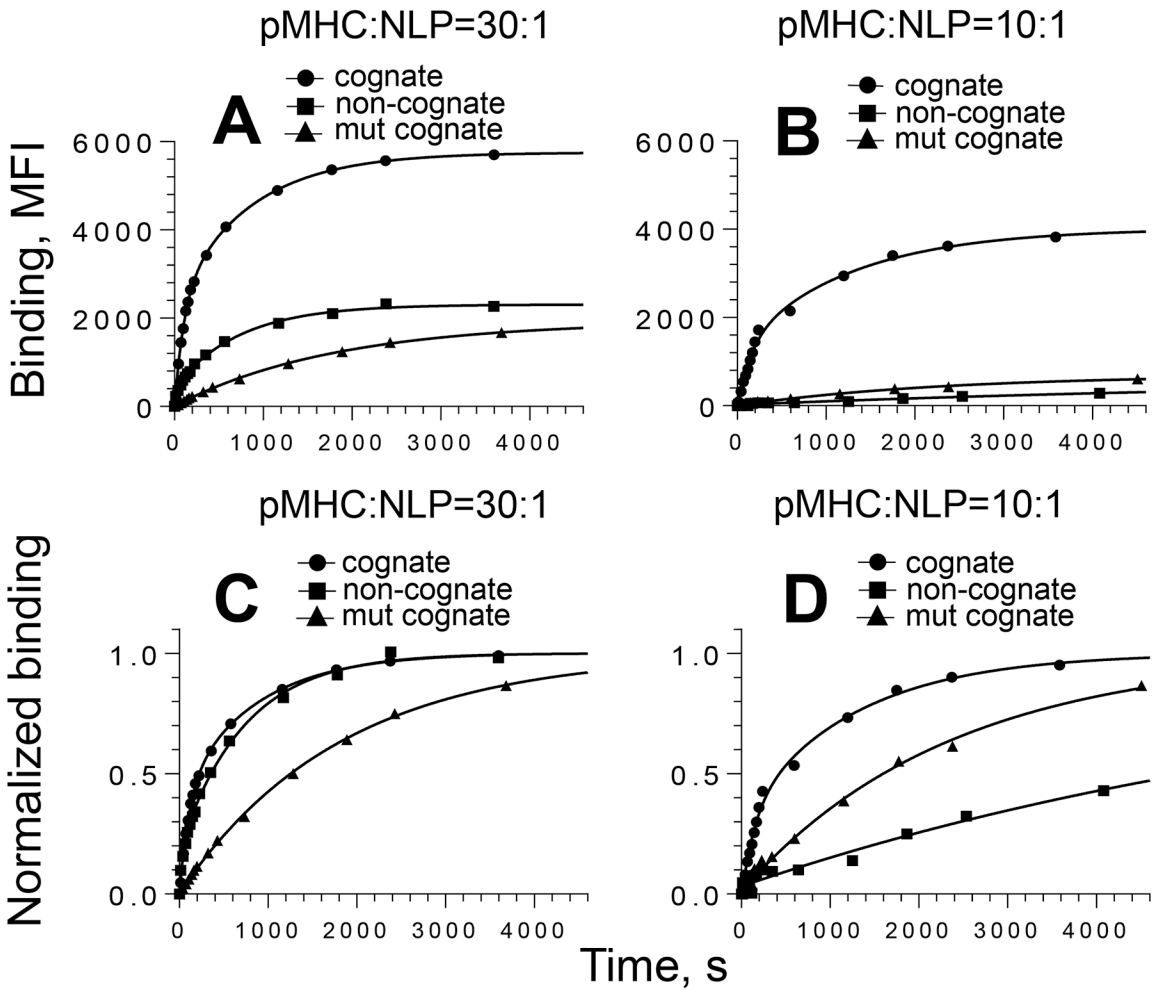

Figure 3. Association kinetics for the binding of pMHC/NiNLPs to the surface of live CTL.

CER-43 $CD8^+$ T cells were mixed with 5 nM pMHC/NiNLP conjugates at 18°C and binding was measured as a function of time by flow cytometry. The experimental data and best fit are shown for strong agonist GL9-HLA-A2/NiNLP (**circle**), non-cognate Tax-HLA-A2/NiNLP (**square**) and cognate GL9-HLA-A2mut/NiNLP (**triangle**) conjugates at pMHC to NiNLP ratios of 30:1 (**A** and **C**) and 10:1 (**B** and **D**). For comparison, normalized data and their fits (**C** and **D**) are presented. Results of representative experiment (N=3) are shown.

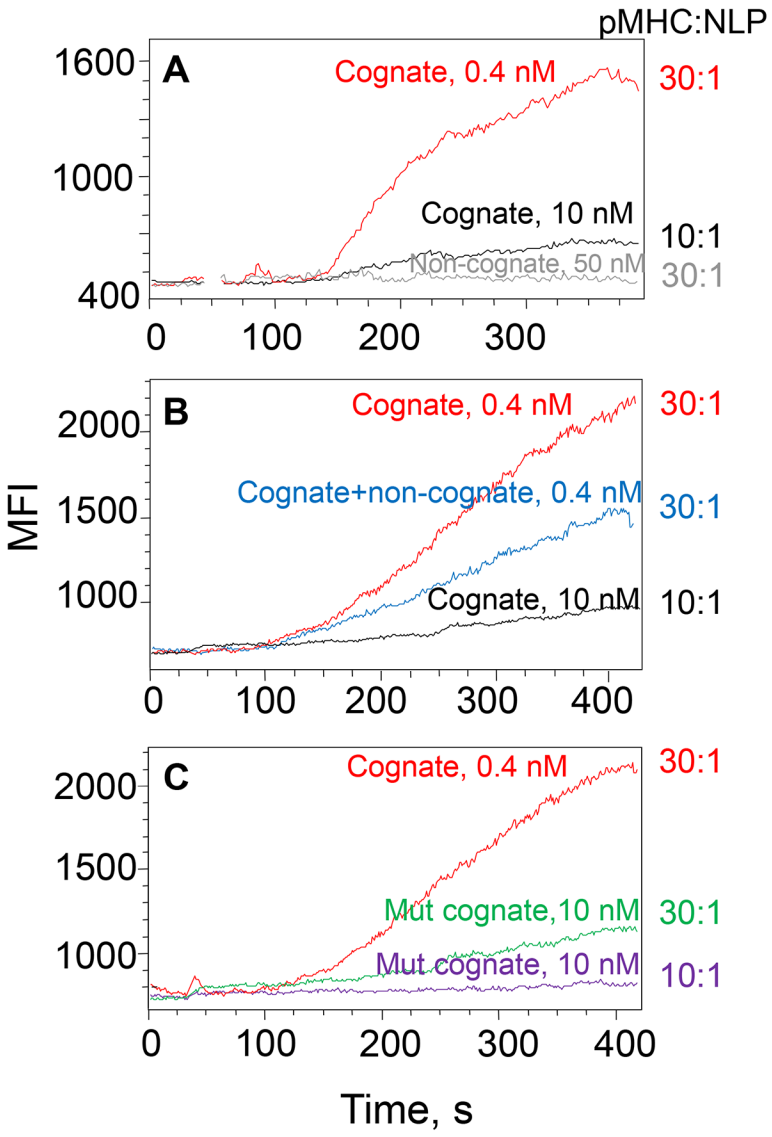

Figure 4. Variations in the kinetics of intracellular Ca^{2+} accumulation in CTL induced by pMHC/NiNLP conjugates with different pMHC density.

Fluo-3 labelled 68A62 $CD8^+$ T cells were mixed with cognate pMHC/NiNLP conjugates at indicated concentrations, and changes in intracellular fluorescent intensity were recorded by flow cytometry. NiNLPs were loaded with: (**A**) 30 (**red**) and 10 (**black**) cognate IV9-HLA-A2 molecules; (**B**) 30 (**red**) or 10 (**black**) cognate IV9-HLA-A2 molecules or mixture of 10 cognate IV9-HLA-A2 molecules and 20 non-cognate Tax-HLA-A2 molecules (**blue**); (**C**) 30 cognate IV9-HLA-A2 molecules (**red**), 30 cognate IV9-HLA-A2mut molecules (**green**) and 10 IV9-HLA-A2mut (**violet**). Data shown are representative from 2 to 4 independent experiments.

Table 1.

Equilibrium binding parameters of low- and high-density pHLA-A2/NiNLPs interacting with live 68A62 cells at 4°C

NiNLP[1)]	pMHC[2)]	Kapp, nM[3)] 4°C	Enhancement factor[4)]	Normalized binding plateau[5)]
5% NiNTA	cognate	4.61±1.96	NA	1
5% NiNTA	non-cognate	9.43±1.81	NA	0.340±0.069
5% NiNTA	cognate, mut	31.2±7.32	NA	0.463±0.005
25% NiNTA	cognate	0.829±0.368	5.6	1
25% NiNTA	non-cognate	0.286±0.116	33	0.390±0.085
25% NiNTA	cognate, mut	5.60±0.509	5.6	0.415±0.010

1) 5% and 25% NiNTA containing NLPs displayed 10 and 30 pMHC molecules per nanoparticle, respectively

2) pMHCs were: IV9-HLA-A2 (cognate), Tax-HLA-A2 (non-cognate), IV9-HLA-A2mut (cognate with mutation in HLA-A2 diminishing interactions with CD8)

3) Kapp, apparent equilibrium binding constants, mean±SD are based on 3 independent experiments (N=3)

4) the ratio between Kapp measured for low- and high-density pHLA-A2/NiNLPs

5) Binding plateau values were measured from the fit of experimental data and normalized relatively the plateau value for the cognate conjugates

Table 2.

Association binding kinetics of 5 nM pMHC/NiNLPs with CER43 T cells at 18°C[1)].

NiNLP[1)]	pMHC[2)]	Association model	τ_{fast}, s[3)]	τ_{slow}, s[3)]	% fast component
5% NiNTA	cognate	two-phase	164±21.6	1301±91	30.5±4.9
	non-cognate	one-phase	831±138	NA	NA
	cognate, mut	one-phase	2310±50.2	NA	NA
25% NiNTA	cognate	two-phase	78.7±35.4	703±178	37.6±5.1
	non-cognate	two-phase	58.1±14.6	831±138	20.6±5.3
	cognate, mut	one-phase	1751±92.6	NA	NA

1)5% and 25% NiNTA containing NLPs displayed 10 and 30 pMHC molecules per nanoparticle, respectively

2)pMHCs were: GL9-HLA-A2 (cognate), Tax-HLA-A2 (non-cognate), GL9-HLA-A2m (cognate with mutation in HLA-A2 diminishing interactions with CD8)

3)τ is time constant in equation 2